Protein Science (1995), *4*:167-177. Cambridge University Press. Printed in the USA.

Early intermediates in the folding of dihydrofolate reductase from *Escherichia coli* detected by hydrogen exchange and NMR

BRYAN E. JONES[1] AND C. ROBERT MATTHEWS

Department of Chemistry, Biotechnology Institute and Center for Biomolecular Structure and Function, The Pennsylvania State University, University Park, Pennsylvania 16802

(RECEIVED August 18, 1994; ACCEPTED November 23, 1994)

Abstract

The kinetic folding mechanism for *Escherichia coli* dihydrofolate reductase postulates two distinct types of transient intermediates. The first forms within 5 ms and has substantial secondary structure but little stability. The second is a set of four species that appear over the course of several hundred milliseconds and have secondary structure, specific tertiary structure, and significant stability (Jennings PA, Finn BE, Jones BE, Matthews CR, 1993, *Biochemistry 32*:3783-3789). Pulse labeling hydrogen exchange experiments were performed to determine the specific amide hydrogens in α-helices and β-strands that become protected from exchange through the formation of stable hydrogen bonds during this time period. A significant degree of protection was observed for two subsets of the amide hydrogens within the dead time of this experiment (6 ms). The side chains of one subset form a continuous nonpolar strip linking six of the eight strands in the β-sheet. The other subset corresponds to a nonpolar cluster on the opposite face of the sheet and links three of the strands and two α-helices. Taken together, these data demonstrate that the complex strand topology of this eight-stranded sheet can be formed correctly within 6 ms. Measurement of the protection factors at three different folding times (13 ms, 141 ms, and 500 ms) indicates that, of the 13 amide hydrogens displaying significant protection within 6 ms, 8 exhibit an increase in their protection factors from ~5 to ~50 over this time range; the remaining five exhibit protection factors >100 at 13 ms. Only approximately half of the population of molecules form this set of stable hydrogen bonds. Thirteen additional hydrogens in the β-sheet become protected from exchange as the set of native conformers appear, suggesting that the stabilization of this network reflects the global cooperativity of the folding reaction.

Keywords: dihydrofolate reductase; folding intermediates; hydrogen exchange; NMR spectroscopy; protein folding

Structural characterization of partially folded forms that appear during protein folding reactions is crucial to the solution of the protein folding problem. Stopped-flow CD spectroscopy (Kuwajima, 1989; Kuwajima et al., 1991; Sugawara et al., 1991) and quench-flow hydrogen exchange methods in combination with NMR spectroscopy (Roder et al., 1988; Udgaonkar & Baldwin, 1988, 1990) have convincingly demonstrated that secondary structure can form within the first few milliseconds of the folding reactions for a variety of proteins (Baldwin & Roder, 1991). Hydrophobic dye binding experiments (Semisotnov et al., 1991; Mann & Matthews 1993; Itzhaki et al., 1994; Jones et al., 1994) show that nonpolar surfaces also form in the same time range. These surfaces probably reflect the association of individual elements of secondary structure through van der Waals interactions between hydrophobic side chains. This supposition is based, in part, upon the absence of organized structure in fragments of proteins or peptides corresponding to many of these elements (Shin et al., 1993; Lumb et al., 1994). The structural and thermodynamical insights provided by the combined use of these techniques have significantly improved the understanding of the earliest events in protein folding.

Although quench-flow hydrogen-exchange NMR techniques have been used to detect native-like hydrogen bonding patterns in early folding intermediates for proteins with all α (cytochrome *c*, Roder et al., 1988; apomyoglobin, Jennings & Wright, 1993), all β (interleukin-1β, Varley et al., 1993), or α + β (ribo-

Reprint requests to: C. Robert Matthews, Department of Chemistry, Biotechnology Institute and Center for Biomolecular Structure and Function, The Pennsylvania State University, University Park, Pennsylvania 16802; e-mail: crm@psuvm.psu.edu.

[1] Present address: University of Washington, Department of Biochemistry, Seattle, Washington 98185.

Abbreviations: 2QF-COSY, double quantum-filtered correlation spectroscopy; DHFR, dihydrofolate reductase from *Escherichia coli*; pH*, uncorrected pH meter reading; ANS, 1-anilinonapthalene-8-sulfonate; MTX, methotrexate.

nuclease A, Udgaonkar & Baldwin, 1988, 1990; barnase, Bycroft et al., 1990; hen lysozyme, Radford et al., 1992; T4 lysozyme, Lu & Dahlquist, 1992; ribonuclease T_1, Mullins et al., 1993; staphylococcal nuclease, Jacobs & Fox, 1994) motifs, there are as yet no such reports for α/β proteins.

Dihydrofolate reductase from *Escherichia coli* offers several advantages for this type of study: (1) DHFR is a member of the α/β class of proteins, containing eight β-strands (seven of which are parallel) and four α-helices (Bolin et al., 1982; Bystroff & Kraut, 1991). Strands βB, βC, and βD and helices αC and αE form a nucleotide-binding domain that is found in most proteins that bind NADH or NADPH as reducing cofactors (Kinemage 1). (2) Extensive optical studies of the folding reaction of DHFR have shown that the protein folds through two different types of intermediates before being converted to native or native-like forms, N_1-N_4, through four parallel channels (Jennings et al., 1993). The burst phase intermediate and the set of related I_1-I_4 intermediates contain substantial secondary structure, as detected by far UV CD spectroscopy (Kuwajima et al., 1991), but cannot bind the tight-binding, competitive inhibitor MTX (Touchette et al., 1986). (3) DHFR has no disulfide crosslinks that would constrain the unfolded protein, e.g., ribonuclease A and lysozyme, nor does it have a covalently bound prosthetic group, e.g., the heme in cytochrome *c*, that could significantly influence the folding pathway. The only information available to direct the folding mechanism is contained in the amino acid sequence. (4) The amide hydrogen NMR assignments are available (Falzone et al., 1990, 1991, 1994), providing potential probes of the secondary structure contained in the strands and helices.

Pulse labeling hydrogen-exchange NMR experiments on DHFR reveal that most, if not all, of the eight-stranded β-sheet can form within 6 ms, consistent with previous stopped-flow CD results (Kuwajima et al., 1991). The observation that only approximately one-half of the molecules significantly protect amide hydrogens in the sheet and two of the helices in this reaction indicates that the formation of parallel pathways in the folding of DHFR occurs at the level of the earliest folding intermediates. These results are similar to those obtained from pulse labeling studies of the folding of hen egg lysozyme (Radford et al., 1992) and suggest that partitioning into folding pathways reflects the initial development of secondary and/or tertiary structure for these two proteins.

Results

Identification of stable hydrogen bonds

The set of amide hydrogens that could serve as useful probes of folding intermediates in DHFR was determined by a simple exchange-out experiment at pH* 6.86 and 25 °C. A lyophilized, fully protonated sample of DHFR containing 1.5 molar excess of folate and appropriate buffer components was dissolved in ^2H_2O and a 2QF-COSY spectrum was recorded immediately. The apo- and MTX binary forms of DHFR have been shown previously to exist in solution as two slowly interconverting conformers (Falzone et al., 1991). The binding of folate simplifies the NMR spectrum, apparently by selectively binding to one of these conformers (Falzone et al., 1990). Folate also serves the useful purpose of stabilizing the native conformation of the protein, limiting hydrogen exchange during sample work-up and NMR analysis.

Following the acquisition of the initial 2QF-COSY spectrum (~12 h), a second spectrum was recorded. Cross peaks for amide hydrogens that did not decrease in intensity by more than 25% in the second spectrum relative to the first were chosen as probes for these experiments (data not shown). This level of retardation of exchange corresponds to protection factors (the intrinsic rate of exchange divided by the observed rate of exchange) in excess of 1.5×10^4. The locations of the 26 residues that satisfy this criterion are shown in Figure 1 and Kinemage 2. Interestingly, only two of these residues reside in α-helices (Ala 81 and Phe 103); all others span the eight-stranded β-sheet.

Kinetics of amide hydrogen protection

The normalized extent of hydrogen exchange (proton occupancy) was measured as a function of time after initiating the refolding reaction to determine the rates at which individual hydrogens become protected during folding. The spectrum of the unfolded control sample, which establishes the relative proton occupancy at zero folding time, $t_f = 0$, is shown in Figure 2A. This spectrum is nearly indistinguishable from the spectrum of freshly dissolved DHFR/folate in ^2H_2O (data not shown), demonstrating that the pulse labeling reactions and sample work-up do not affect the native structure of DHFR in any detectable manner.

Significant decreases in the intensities of cross peaks can be observed in the spectrum of the sample obtained with a folding time equivalent to the fastest instrumental mixing time (t_f = 6 ms; Fig. 2B). As the folding time is increased, the intensities of all cross peaks decrease progressively. At a folding time of 500 ms (Fig. 2C), it is evident that not all of the amide hydrogens are protected to the same extent. Some cross peaks are almost nonexistent (those highlighted in Fig. 2C), whereas others still show significant intensity. This differential behavior suggests that the folding intermediates in DHFR selectively stabilize certain amide hydrogen bonds; the remaining hydrogen bonds apparently become stabilized only when the native conformers appear.

Owing to aggregation at acidic pH values, a pH* of 6.3 was used for both the refolding and quench steps. The intrinsic amide hydrogen exchange rate at this pH ($\tau \cong 1$ s) is more rapid than some of the slower folding steps ($\tau \geq 10$ s; Touchette et al., 1986; Jennings et al., 1993), making it impossible to obtain useful information on protection at longer folding times. This precludes the possibility of discriminating the hydrogens that become protected in slower reactions from those that are susceptible to washout in the quench step.

A necessary control for the pulse labeling experiment is the determination of amide hydrogens that are susceptible to exchange either during the quench or the sample work-up. This control was performed by maintaining the sample at pH* 6.3 during the folding and pulse steps, each with a duration of 20 ms. Under these conditions (pH* 6.3 and 15 °C), only those probes that become protected with rates much slower than the intrinsic rate of exchange ($\tau \cong 1$ s) will exchange with the excess hydrogen in the solvent and exhibit crosspeaks in the NMR spectrum. The spectrum of this sample (Fig. 2D) shows a small number of cross peaks, all with significantly reduced intensities compared to the unfolded control. These particular amide hydrogens only become fully protected in one of the slower folding steps because no crosspeaks are observed in the NMR spectrum of the native control sample (data not shown).

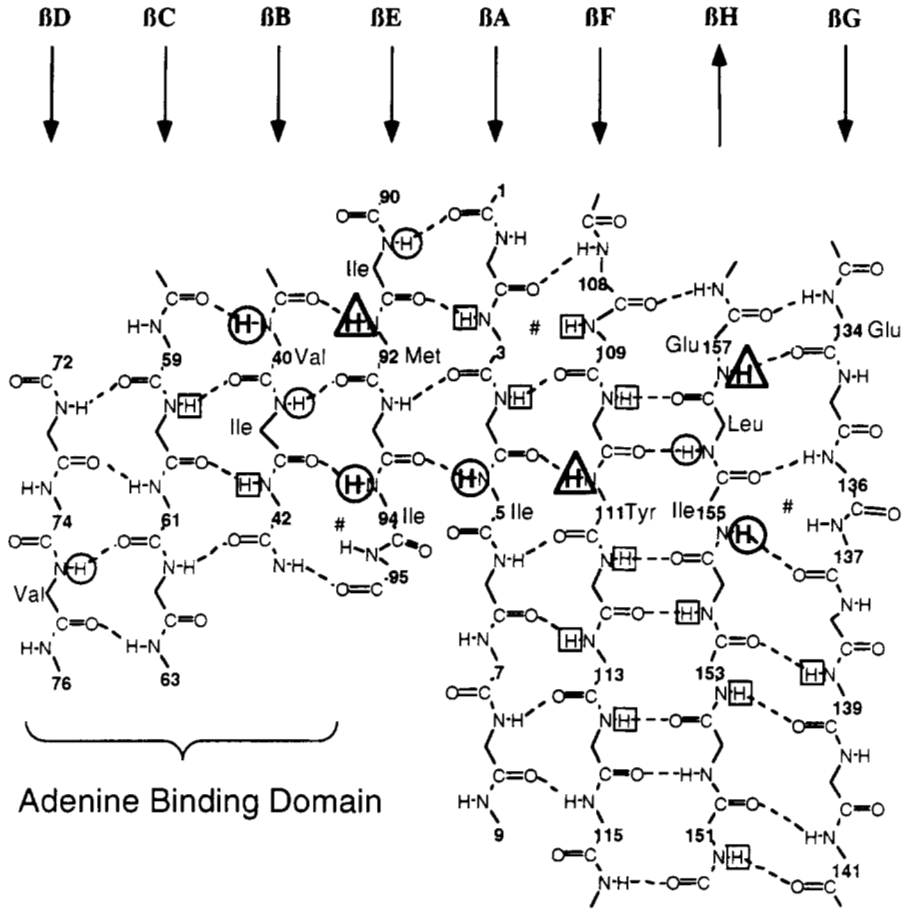

Fig. 1. Schematic of the hydrogen bonding network for the β-sheet of DHFR, based on the crystal structure of the MTX:DHFR binary complex (Bolin et al., 1982), indicating probes used in the pulse labeling experiments. Residue numbers indicate positions whose side chains protrude from the same side of the β-sheet. Circles indicate Class 1 amide hydrogens (weakly protected within 13 ms), triangles indicate Class 2 hydrogens (strongly protected within 13 ms), and boxes indicate the probes that form Class 3 (not protected within 13 ms); those shown in bold are from residues whose side chains are on the same side of the β-sheet. The two probes used in this study that are not shown, Ala 81 and Phe 103, are in α-helical segments. The locations of β-bulges that interrupt the normal hydrogen bonding pattern are indicated (#).

Plots of proton occupancy versus folding time are shown in Figure 3 for representative β-strand residues in the adenine binding domain (βB, βC, and βD; Fig. 3A), the major domain (βA and βE–βH, Fig. 3B), and the two residues in α-helices (Fig. 3C). Typically, the normalized proton occupancies obtained from two different samples with identical preparation agreed within 10%. When the proton occupancies as a function of t_f are fit to a single exponential term plus a constant, the apparent relaxation times vary from 0.16 s to 2.0 s (Table 1). The constant term was included in these fits to reflect the additional folding phases that are detected in optical studies of folding (Jennings et al., 1993). The estimated errors in these values are sufficiently large that the possibility that they all reflect a common process with a relaxation time of approximately 0.5 s cannot be excluded. It is also possible that the protection is determined by more than a single folding phase. The τ_4 and τ_5 folding phases for DHFR occur in this time range (Jennings et al., 1993); $\tau_4 = 1.05 \pm 0.06$ s and $\tau_5 = 100 \pm 8$ ms under these conditions as measured by stopped-flow fluorescence spectroscopy (data not shown).

The less-than-unitary amplitude for the proton occupancy at 6 ms for most of these amide hydrogens (Fig. 3A,B,C; Table 1) suggests that stable hydrogen bonds are also forming within the dead time of mixing. However, given the magnitude of the statistical error in the fits, the extrapolation to $t_f = 0$ for the purposes of determining the extent of protection occurring within the dead time of mixing is not warranted. A more reliable method of obtaining this information is by measurement of the protection factors (see below).

Three probes, Glu 139, Tyr 151, and Phe 153, were protected too slowly for their relaxation times to be measured accurately under these conditions; the deuterium initially present exchanges with hydrogen while the protein continues to fold during the quench step. Based upon fits of the available data, the relaxation times for the protection of these three amide hydrogens must be greater than 2 s. Consistent with this slow protection is the observation of cross peaks for these same amide hydrogens in the low pH control (Fig. 2D).

Measurement of protection factors

Inspection of the data in Figure 3 and Table 1 reveals that the proton occupancy after 6 ms is significantly less than 1 for several of the probes, e.g., Val 40, Ile 91, Ala 81, and Phe 103. Such behavior indicates that these amide hydrogens and several others (data not shown) can form stable hydrogen bonds within the dead time of the experiment. What is not clear from these data is whether only a fraction of the population is capable of forming these hydrogen bonds or whether the pH of the exchange pulse, pH* 9.5, was insufficient to completely exchange all of the amide hydrogens at these positions. This issue can be resolved by measuring the proton occupancy as the intensity of the exchange pulse is varied. The variation of the pulse inten-

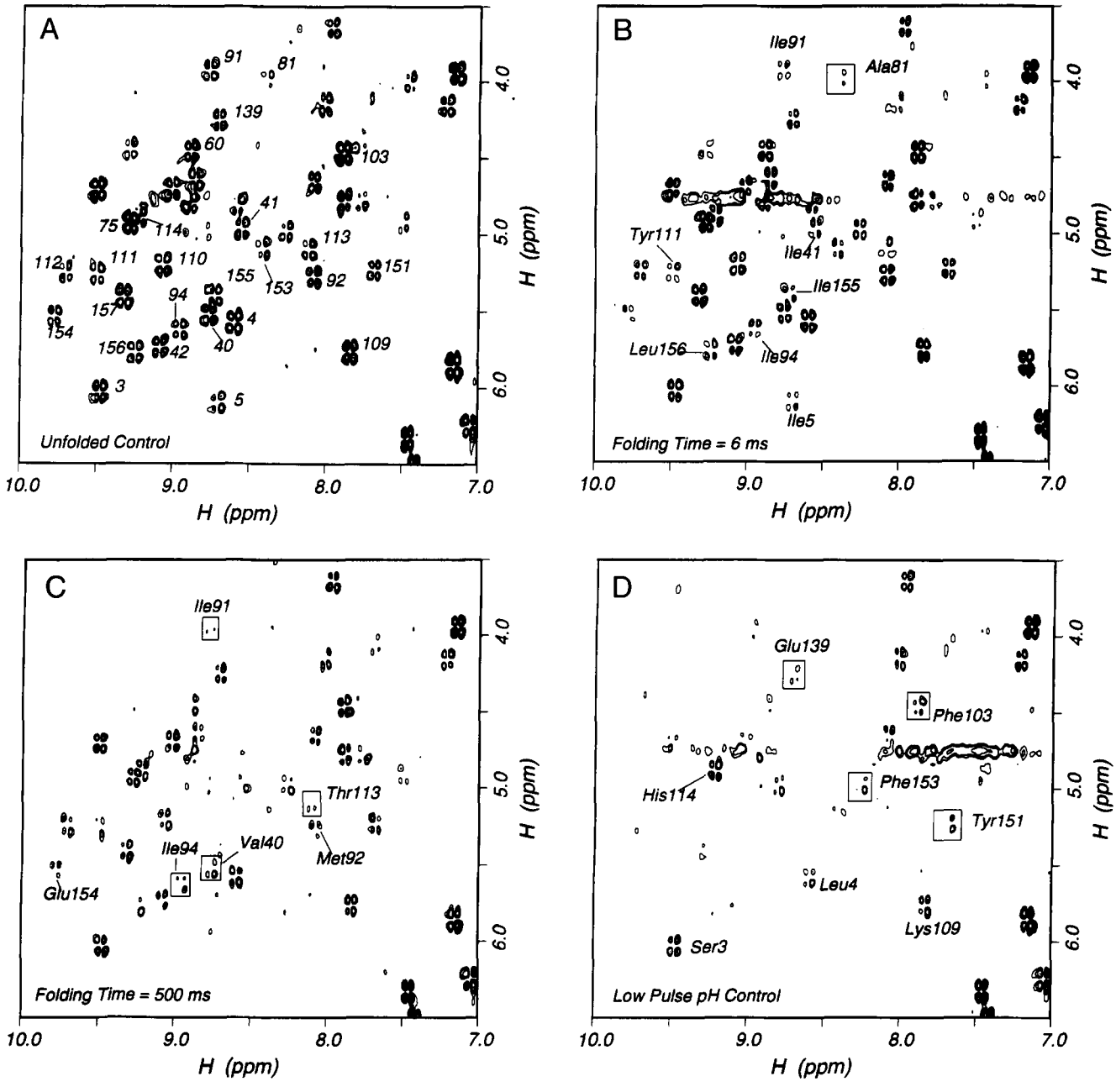

Fig. 2. 2QF-COSY spectra of pulse labeling samples with **(A)** $t_f = 0$ (unfolded control, **(B)** $t_f = 6$ ms, **(C)** $t_f = 500$ ms, and **(D)** the low pH pulse control. Residues indicated are discussed in the text. 2QF-COSY spectra were acquired on a Bruker AM-500 and typically required ~12 h for data acquisition.

sity by varying the pH of the exchange reaction also permits a quantitative measurement of the protection factor (Elöve & Roder, 1991; Englander & Mayne, 1992).

The pulse intensity was varied at 13 ms, 141 ms, and 500 ms to measure the populations and protection factors of three different species that appear during the folding of DHFR (Jennings et al., 1993). At 13 ms, the most highly populated species is the burst phase intermediate; the set of I_1-I_4 intermediates comprises ~12% and the N_4 conformer less than 1% of the population. At 141 ms, the I_1-I_4 intermediates comprise ~70% of the population, and the N_4 conformer is ~4%. At 500 ms, the N_4 conformer is significantly populated (~25%). The proton occupancies as a function of pH for the 26 amide hydrogen probes displayed three different classes of behavior; representative examples are shown in Figure 4. For the first class, illustrated by Val 40, the proton occupancies show a significant dependence on the pH of the exchange pulse (Fig. 4A). The sigmoidal shape reflects the resistance of these amide hydrogens to exchange at lower pH (pH* 8.5) and their nearly complete exchange at higher pH as the intrinsic rate of exchange accelerates at alkaline pH. A similar pH dependence is observed at 141 and 500 ms (Fig. 4A), with the exception that the transitions are

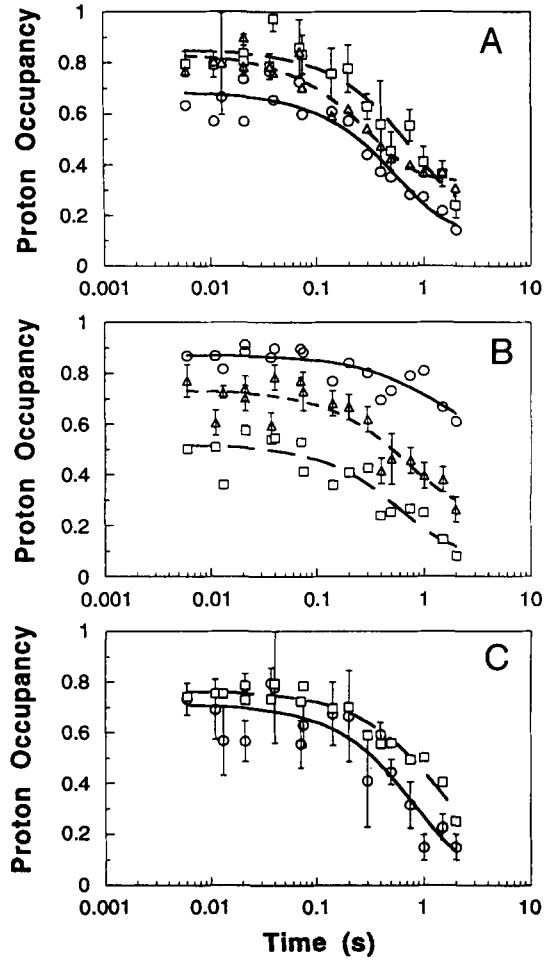

Fig. 3. Plots of proton occupancy versus folding time for representative amino acids throughout the structure of DHFR. **A:** Residues from β-strands in the adenine binding domain (strands βB-βD) include Val 40 (circles), Ile 60 (squares), and Val 75 (triangles). **B:** Residues from β-strands in the major domain (βA, βE-βH) include Ser 3 (circles), Ile 91 (squares), and Glu 157 (triangles). **C:** Two residues that reside in α-helices are Ala 81 (circles) and Phe 103 (squares). Data points are the average of integrations from spectra of two samples with identical preparations; error bars indicate standard deviations. Proton occupancy values were obtained by normalizing the values of the integrations of the absolute volume of the phase-sensitive crosspeaks to the volumes of three non-exchanging crosspeaks in the aromatic region of the 2QF-COSY spectra and to the volumes of crosspeaks in the spectra of the unfolded and native controls.

Table 1. *Relaxation times, amplitudes, and extent of protection at 6 ms for the amide hydrogens during refolding*

Residue	Location	Relaxation time (s)	Amplitude[a]	Protection at 6 ms[b]
Ser 3	βA	1.3 ± 0.9[c]	0.3 ± 0.1	0.13 ± 0.20
Leu 4	βA	0.5 ± 0.2	0.20 ± 0.04	0.12 ± 0.08
Ile 5	βA	0.4 ± 0.1	0.40 ± 0.05	0.34 ± 0.9
Val 40	βB	0.6 ± 0.1	0.54 ± 0.04	0.32 ± 0.08
Ile 41	βB	0.4 ± 0.1	0.52 ± 0.04	0.22 ± 0.07
Met 42	βB	0.4 ± 0.1	0.43 ± 0.04	0.13 ± 0.10
Ile 60	βC	0.83 ± 0.02	0.64 ± 0.07	0.15 ± 0.14
Val 75	βD	0.32 ± 0.05	0.49 ± 0.03	0.19 ± 0.05
Ala 81	αE	0.6 ± 0.2	0.60 ± 0.07	0.29 ± 0.14
Ile 91	βE	0.8 ± 0.3	0.44 ± 0.05	0.50 ± 0.10
Met 92	βE	0.34 ± 0.06	0.52 ± 0.04	0.20 ± 0.07
Ile 94	βE	0.6 ± 0.1	0.58 ± 0.06	0.26 ± 0.12
Phe 103	αF	1.7 ± 0.6	0.7 ± 0.1	0.23 ± 0.08
Lys 109	βF	0.9 ± 0.5	0.35 ± 0.09	0.13 ± 0.18
Leu 110	βF	1.0 ± 0.4	0.6 ± 0.1	0.10 ± 0.20
Tyr 111	βF	0.23 ± 0.08	0.39 ± 0.05	0.23 ± 0.09
Leu 112	βF	1.4 ± 0.8	0.7 ± 0.2	0.10 ± 0.30
Thr 113	βF	0.7 ± 0.3	0.45 ± 0.08	0.13 ± 0.15
His 114	βF	0.16 ± 0.07	0.35 ± 0.05	0.14 ± 0.08
Glu 139	βG	>2	nd	<0.10[d]
Tyr 151	βH	>2	nd	<0.10[d]
Phe 153	βH	>2	nd	<0.10[d]
Glu 154	βH	1.1 ± 0.7	0.5 ± 0.1	0.10 ± 0.15
Ile 155	βH	2.0 ± 0.8	0.8 ± 0.3	0.20 ± 0.07
Leu 156	βH	1.3 ± 0.5	0.7 ± 0.1	0.30 ± 0.13
Glu 157	βH	0.7 ± 0.3	0.46 ± 0.06	0.27 ± 0.13

[a] Amplitude is in units of proton occupancy.
[b] Normalized extent of protection at the mixing dead time of these experiments by extrapolation of the kinetic data (taken with a pulse pH* of 9.5).
[c] Errors are the standard deviations obtained from nonlinear least-squares fitting of the data to a single exponential plus a constant.
[d] Values are estimated from linear extrapolation of data over the first 100 ms.

shifted to higher pH values. This shift is indicative of an increase in protection factor as folding time increases.

These data can be fit to an equation to determine both the protection factor and the population of molecules displaying this protection (Elöve & Roder, 1991):

$$P(\text{pH}) = (1 - f) + (f \times \{1 - \exp[-(k_c/pf) \times t_p]\}), \quad (1)$$

where $P(\text{pH})$ is the observed proton occupancy as a function of pH, k_c is the base-catalyzed intrinsic hydrogen exchange rate, pf is the observed protection factor, f is the fraction of molecules displaying protection factor pf, and t_p is the pulse duration. Because the pulse pH is well above pH 3, the intrinsic rate constant for exchange can be expressed as a function of pH as:

$$k_c(\text{pH}) = k_{OH} \cdot 10^{(\text{pH}-\text{pK}_W)}, \quad (2)$$

where k_{OH} is the second-order rate constant for base-catalyzed exchange calculated for an amide hydrogen and pK_W is 14.53 at 15 °C (Bai et al., 1993). The value of k_{OH} depends upon the nearest neighbors in the amino acid sequence (Bai et al., 1993).

The results of nonlinear least-squares fits of these data to Equation 1 are shown in Table 2. The protection factors for Ile 5, Val 40, Ile 41, Val 75, Ile 91, Ile 94, Ile 155, and Leu 156 are all very similar and have an average value of 5 after 13 ms. The protection factors increase to an average of 18 after 141 ms and an average of 48 after 500 ms. The fits also show that these titrations do not range from a proton occupancy of 0 to a proton occupancy of 1 as would be expected if the entire population of molecules were exhibiting this degree of protection at

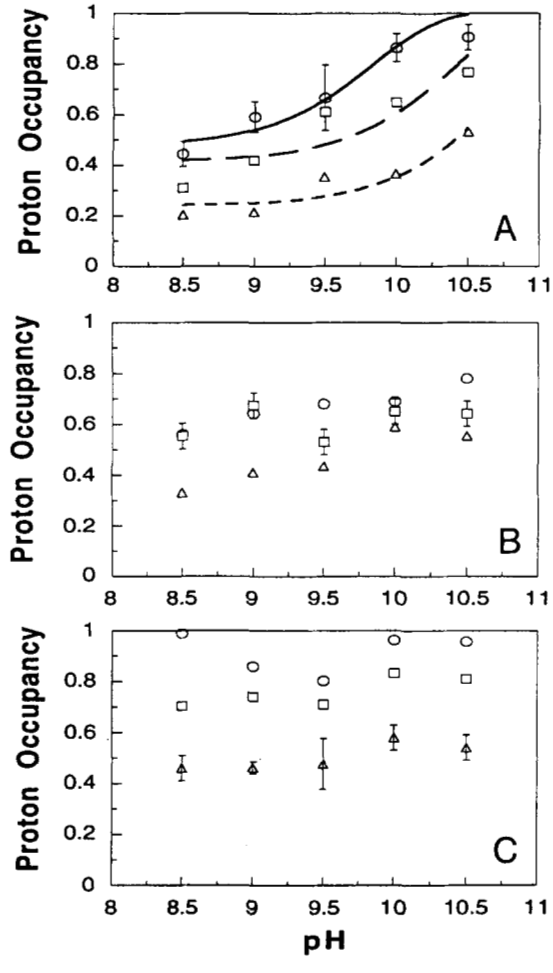

Fig. 4. Plots of proton occupancy versus pulse pH for each of the three classes of protection behavior observed. **A:** Class 1, Val 40. **B:** Class 2, Tyr 111. **C:** Class 3, Met 42. Individual points are the average of data obtained from two samples; error bars indicate standard deviations. Lines drawn for Val 40 in A are fits of the data to Equation 1 (see Results). Pulse duration was maintained constant at 20 ms for each of the indicated folding times: 13 ms (circles), 141 ms (squares), and 500 ms (triangles).

these amide hydrogens. The amplitude of this phase has an average value of 0.59 ± 0.07 at both 13 ms and 141 ms for this class of hydrogens (Table 2). This suggests that only 59% of the population is protecting this set of amide hydrogens in both the burst phase intermediate and the set of I_1-I_4 intermediates. The fraction increases to 70% at 500 ms, presumably reflecting the formation of the N_4 native conformer (Jennings et al., 1993).

The second class of behavior is exhibited by Tyr 111 in Figure 4B. The proton occupancy for this group of hydrogens, which include Ala 81, Met 92, Phe 103, Tyr 111, and Glu 157, is significantly less than 1 at 13 ms. In the case of Tyr 111, the occupancy is ~0.75 at a pulse pH* of 9.5 and displays no significant dependence upon pH. The lack of a dependence upon pH indicates that the protection factors must be >100, based upon the data collected at pH* 10.5. Data were not taken at higher pH values to avoid complications arising from alkaline unfolding of the native protein (P.A. Jennings & C.R. Matthews, unpubl. results). The decrease in proton occupancy at longer folding times indicates a larger fraction of the protein protects these amide hydrogens from exchange. The relative populations protecting the probes in this class of hydrogens, calculated from the average of the proton occupancies at pulse pH* values of 9, 9.5, and 10, are shown in Table 2. The increase in population presumably also reflects the formation of the N_4 conformer.

The third class of behavior, displayed by the remaining 13 residues including Met 42 (Fig. 4C), is similar to the second in terms of a lack of pH dependence of the proton occupancy. However, this class is different in that there is no significant protection occurring at 13 ms (Table 2). This class is also similar to the second in that the proton occupancy decreases as folding time increases. The increase in the population with protection factors >100 once again appears to reflect the formation of the native-like, N_4, conformer. Although this classification scheme is qualitative, it does serve to emphasize the differences between the types of protection experienced by different groups of amide hydrogens in the early stages of folding of DHFR.

The locations of the residues in each class are shown in Figure 1. The 13 side chains whose amide hydrogens exhibit significant protection at 13 ms, i.e., members of Class 1 or 2, form two distinct clusters in DHFR: a strip across the center of strands βB, βE, βA, βF, βH, and βG, which also extends to the aminotermini of βB, βC, and βE, and a second hydrophobic cluster around Val 75 on the opposite face of the sheet (Fig. 5; Kinemage 3). The side chains from Ala 81 and Phe 103 that are found on the hydrophobic faces of helices αE and αF, respectively, also form a part of the second cluster. These data demonstrate that the correct topology of the strands in the β-sheet can be achieved within 6 ms after the initiation of refolding. The side chains of the 13 hydrogens that only become significantly protected as the native conformers form, i.e., the members of Class 3, are distributed throughout the β-sheet.

Discussion

Burst phase intermediate

A previous characterization of the burst phase intermediate for DHFR by stopped-flow CD spectroscopy indicated that the secondary structure content is significant and consists primarily of the β-sheet motif (Kuwajima et al., 1991). The present observation of one or more protected amide hydrogens between each of the eight strands for approximately 60% of the population (Fig. 1) strongly suggests that the order of the strands found in native DHFR can be achieved within 6 ms. This is a remarkable finding considering that the strands in DHFR have a complex topology, +2x +1x +1x −3x −2x −2x +1x (Fig. 1; Bolin et al., 1982). These results, along with others on proteins containing antiparallel β-sheet (Briggs & Roder, 1992; Varley et al., 1993), all α-helical (Roder et al., 1988; Jennings & Wright, 1993), and α + β motifs (Udgaonkar & Baldwin, 1988, 1990; Bycroft et al., 1990; Lu & Dahlquist, 1992; Radford et al., 1992; Mullins et al., 1993; Jacobs & Fox, 1994), show that all of the basic protein motifs can form within a few milliseconds from a random coil. New techniques, e.g., photo-initiated refolding (Jones et al., 1993) are required to access the earliest events in folding, which evidently occur in the submillisecond time range.

Table 2. *Protection factors and fractional populations at different folding times for amide hydrogens in DHFR*

		13 ms		141 ms		500 ms	
Residue	Class	P.F.[a]	Pop.[b]	P.F.	Pop.	P.F.	Pop.
Ser 3	3	np[c]	0.08 ± 0.08	>100[d]	0.11 ± 0.09	>100	0.20 ± 0.06
Leu 4	3	np	0.08 ± 0.09	>100	0.15 ± 0.06	>100	0.25 ± 0.10
Ile 5	1	5 ± 1	0.55 ± 0.06	22 ± 5	0.55 ± 0.08	53 ± 10	0.69 ± 0.06
Val 40	1	5 ± 2	0.53 ± 0.06	17 ± 6	0.59 ± 0.07	42 ± 9	0.64 ± 0.03
Ile 41	1	2.0 ± 0.8	0.63 ± 0.09	25 ± 8	0.46 ± 0.06	80 ± 12	0.61 ± 0.03
Met 42	3	np	0.12 ± 0.08	>100	0.24 ± 0.06	>100	0.49 ± 0.06
Ile 60	3	np	0.14 ± 0.09	>100	0.18 ± 0.09	>100	0.30 ± 0.09
Val 75	1	3.0 ± 0.8	0.51 ± 0.09	15 ± 3	0.51 ± 0.06	61 ± 13	0.64 ± 0.05
Ala 81	2	>100	0.24 ± 0.15	>100	0.40 ± 0.10	>100	0.60 ± 0.05
Ile 91	1	5.0 ± 0.8	0.78 ± 0.04	9 ± 1	0.80 ± 0.05	42 ± 8	0.77 ± 0.03
Met 92	2	>100	0.21 ± 0.02	>100	0.35 ± 0.02	>100	0.60 ± 0.06
Ile 94	1	4 ± 1	0.48 ± 0.08	10 ± 2	0.45 ± 0.05	24 ± 5	0.66 ± 0.04
Phe 103	2	>100	0.24 ± 0.10	>100	0.30 ± 0.03	>100	0.48 ± 0.05
Lys 109	3	np	0.13 ± 0.08	>100	0.19 ± 0.06	>100	0.31 ± 0.05
Leu 110	3	np	0.04 ± 0.03	>100	0.15 ± 0.05	>100	0.40 ± 0.10
Tyr 111	2	>100	0.33 ± 0.02	>100	0.38 ± 0.07	>100	0.52 ± 0.08
Leu 112	3	np	0.13 ± 0.09	>100	0.19 ± 0.13	>100	0.27 ± 0.06
Thr 113	3	np	0.13 ± 0.10	>100	0.16 ± 0.06	>100	0.30 ± 0.15
His 114	3	np	0.12 ± 0.08	>100	0.22 ± 0.15	>100	0.40 ± 0.09
Glu 139	3	np	0.09 ± 0.06	>100	0.16 ± 0.08	>100	0.33 ± 0.08
Tyr 151	3	np	0.04 ± 0.08	>100	0.06 ± 0.08	>100	0.16 ± 0.06
Phe 153	3	np	0.06 ± 0.12	>100	0.16 ± 0.09	>100	0.39 ± 0.11
Glu 154	3	np	0.12 ± 0.09	>100	0.22 ± 0.14	>100	0.36 ± 0.08
Ile 155	1	11 ± 3	0.60 ± 0.07	17 ± 4	0.71 ± 0.08	47 ± 5	0.81 ± 0.03
Leu 156	1	9 ± 3	0.62 ± 0.09	28 ± 5	0.64 ± 0.05	54 ± 9	0.78 ± 0.06
Glu 157	2	>100	0.25 ± 0.04	>100	0.33 ± 0.03	>100	0.52 ± 0.03

[a] Protection factor is defined as the ratio of the intrinsic rate of exchange in an unstructured polypeptide to the observed rate of hydrogen exchange. The intrinsic exchange rate was calculated on the basis of the local amino acid sequence using the data of Bai et al. (1993). Errors indicated are standard deviations from nonlinear least-squares fitting of the pulse pH* variation data to the equation described by Elöve and Roder (1991).

[b] Fractional population of protein that displays the indicated protection factor. For Class 2 and Class 3 hydrogens, the population was estimated from the average proton occupancies at pulse pH* values of 9, 9.5, and 10; errors indicate the standard deviations.

[c] Not protected.

[d] Protection factors could not be measured for Class 2 and Class 3 hydrogens due to lack of pH dependence over the range tested and are estimated to be >100.

Seven of the 11 highly protected amide hydrogens in the β-sheet, Ile 5, Val 40, Met 92, Ile 94, Tyr 111, Ile 155, and Glu 157, protrude from the same side and form a continuous, nonpolar network that links five of the internal strands (βB-βE-βA-βF-βH; Fig. 5). Note that only the aliphatic part of the Glu 157 side chain is involved. Ile 41, Val 75, Ile 91, and Leu 156 protrude from the opposite face of the sheet. The protection afforded to Leu 156 may reflect to some extent that observed for Ile 155 and Glu 157. The side chains of Ile 41, Val 75, and Ile 91 contact those of Ala 81 and Phe 103, suggesting that a second

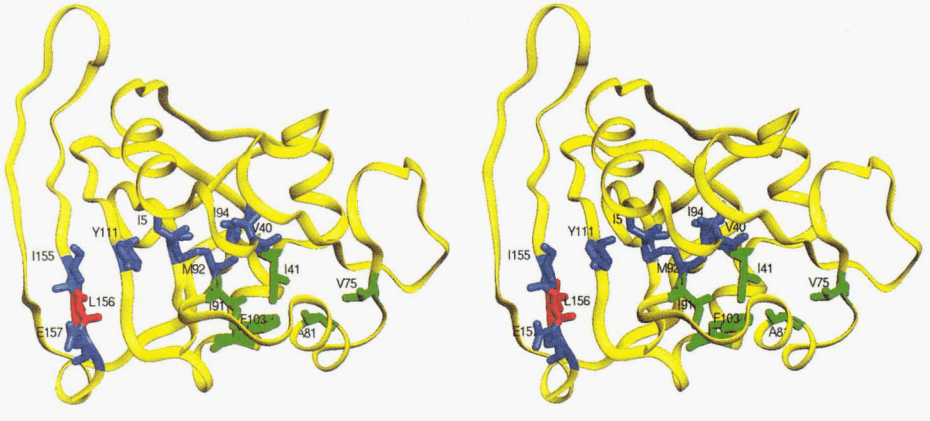

Fig. 5. Location of residues that form the two hydrophobic clusters in the burst phase intermediate. Side chains forming the larger cluster, i.e., Ile 5, Val 40, Met 92, Ile 94, Tyr 111, Ile 155, and Glu 157, are shown in blue, and those forming the smaller cluster, i.e., Ile 41, Val 75, Ala 81, Ile 91, and Phe 103, are shown in green.

cluster of hydrophobic residues on the opposite side of the β-sheet also provides protection in the burst phase intermediate.

A similar observation on the early appearance of hydrophobic clusters has been made in pulse labeling studies of hen lysozyme (Radford et al., 1992). As suggested by these experimenters, the retardation in exchange for the associated amide hydrogens in DHFR may reflect difficulties of solvent penetration into such clusters as well as the formation of stable hydrogen bonds. The existence of a partially developed hydrophobic core early in folding has also been proposed for ubiquitin, a β-sheet protein (Khorasanizadeh et al., 1993).

The existence of clusters of nonpolar side chains in the burst phase intermediate for DHFR offers a potential explanation for the binding of the hydrophobic dye, ANS, during the folding reaction (Jones et al., 1994). When the hydrogen-exchange NMR and ANS binding results are considered together, they suggest that the concerted formation of a hydrogen bonding network and a hydrophobic core(s) may be a critical early event in the folding of β-sheet-containing proteins. Faster folding techniques are required to determine if one of these types of structures proceeds the other in the very earliest stages of folding.

The above hydrophobic clusters assume added significance when compared to others that exist in the native form but are not sufficiently stable to provide protection against exchange. For example, the side chains of Leu 4, Ala 6, Leu 8, Leu 110, and Leu 112 form another cluster on the same face as the smaller of the above clusters. However, none of the Leu 4, Leu 110, and Leu 112 probes indicate protection in the burst phase. Thus, not all hydrophobic clusters are sufficiently stable to provide protection of their amide hydrogens against exchange with solvent in the first few milliseconds of folding.

An intriguing aspect of the two stable clusters that appear early in the folding of DHFR is the high proportion of side chains with branched β carbons. Seven of the 13 side chains are either Ile or Val, four in the larger cluster and three in the smaller (Fig. 5). One possible explanation is the constraint that the branched β carbon places upon the side-chain rotamer populations in the unfolded protein and in a β-strand conformation. Steric restrictions would be minimized and the entropy penalty for folding reduced when an extended β structure is formed, rather than alternatives such as the α-helix (Creamer & Rose, 1992, 1994; Bai & Englander, 1994). Whatever the molecular explanation, measurements of the β-strand propensity for naturally occurring side chains (Kim & Berg, 1993; Minor & Kim, 1994; Smith et al., 1994) have shown that Ile and Val contribute more to the stability of fully folded proteins containing these residues at test β positions than Ala or Leu. Thus, it seems quite likely that branched β-carbon side chains would have a similar effect on partially folded intermediates containing β-strands. The absence of branched β carbons for the Leu 4, Ala 6, Leu 8, Leu 110, and Leu 112 cluster, which does not offer measurable protection against exchange, is also consistent with this hypothesis.

I_1–I_4 intermediates

The observation of one type of intermediate that can protect its amide hydrogens against exchange (Classes 1 and 2; Table 2) and another that cannot (Class 3) after 141 ms is extremely interesting in light of previous optical studies on the folding of DHFR (Kuwajima et al., 1991). Stopped-flow CD studies in conjunction with site-directed mutagenesis demonstrated that Trp 47 and Trp 74 attain a native-like packing in the I_1–I_4 intermediates that appear during this time period. This conclusion was based upon the detection of an exciton coupling between these aromatic side chains, an interaction that is sensitive to the distance and orientation of the two chromophores (Cantor & Schimmel, 1980). Because the magnitude of this coupling in the I_1–I_4 intermediates is identical to that found in the fully folded protein, the entire population of intermediates is very likely to contain this element of specific tertiary structure. The formation of this interaction in the entire population of protein has been confirmed recently with time-resolved fluorescence techniques (Jones et al., 1995).

A native-like tertiary interaction between residues that are separated by 27 positions in the sequence suggests that the adenine binding domain that contains these residues is folded, at least to some extent. Preliminary studies on a fragment of DHFR encompassing residues 37–107, including the adenine binding domain, show that the isolated fragment does not fold to any significant extent (C.V. Gegg & C.R. Matthews, unpubl. results). Therefore, it is quite possible that both the adenine binding domain and the larger domain are folded and associated in the entire population of I_1–I_4 intermediates. The absence of protection against exchange for approximately 40% of this population could mean that this fraction of the protein forms non-native hydrogen bonds or non-native tertiary interactions, either of which might require disruption of the β-sheet to allow access to the native conformation. Exchange of amide hydrogens would then occur during the work-up. Note that the difference between the average fractional amplitudes of the Class 1 and Class 2 hydrogens (Table 2) at the various time points suggests that there are at least two different populations of protein that protect these amide hydrogens.

Another interesting aspect of the development of the I_1–I_4 intermediates from the burst phase species is that no additional amide hydrogens are protected against exchange. The protection factors for the eight amide hydrogens that can be accurately measured, i.e., those in Class 1, however, do increase uniformly. If the enhanced protection factors are taken as indicators of the increased stability of these intermediates (Elöve & Roder, 1991; Englander et al., 1992), then it appears that this stability derives from the formation of tertiary structure, e.g., the Trp 47/Trp 74 contact, and not from extensions of the secondary structure network. These results are also consistent with stopped-flow CD studies that show that no changes in secondary structure are apparent in this time range (Kuwajima et al., 1991). Thus, the driving force in folding at this stage may be the formation of van der Waals interactions and the consequent loss of water from nonpolar side chains.

Udgaonkar and Baldwin (1990) have also noted an increase in the protection factors of several amide hydrogens during the first few hundred milliseconds of folding of ribonuclease A. The absence of protection for additional hydrogens suggests that the progressive increase in the apparent stability of folding intermediates may, in general, reflect the formation of enhanced van der Waals contacts between side chains.

Later events in folding

Stopped-flow CD studies have demonstrated that the four rate-limiting steps in each channel that lead to native or native-like conformers, N_1–N_4, involve further changes in the secondary

structure (Kuwajima et al., 1991). Unfortunately, limitations concerning the solubility of DHFR at acidic pH values preclude the possibility of obtaining hydrogen-exchange NMR data beyond the first few seconds of folding. The observation that half of the probes for DHFR only become protected in slower folding reactions is, however, consistent with the further development of secondary structure in longer time ranges (Kuwajima et al., 1991). Because these slower reactions lead to native or native-like conformers, the protection of these probes must require the global cooperativity of the folding reaction.

Parallel folding pathways

DHFR has been shown to fold through four parallel channels whose interconversions are slower than folding to four native or native-like conformers (Jennings et al., 1993). These channels were proposed to appear at the stage where the I_1–I_4 intermediates become populated, i.e., after the first few hundred milliseconds. The pulse labeling NMR results presented in this communication suggest that the origin of the separate pathways occurs even earlier. The observation of (at least) two distinct populations of protein, one that is capable of providing significant protection against exchange and one that is not, implies that separate channels can form within 6 ms. This heterogeneity remains beyond hundreds of milliseconds, demonstrating that the differences in protection, i.e., structure and/or stability, exist until the native conformers are formed.

Separate pathways have been also observed in the folding of hen egg lysozyme (Radford et al., 1992) and ribonuclease A (Udgaonkar & Baldwin, 1990). An attractive explanation is a slow *cis/trans* isomerization of peptide bonds within the polypeptide chain, particularly at Xaa–Pro peptide bonds (Brandts et al., 1975). Proline isomerization has been shown to play a role in causing separate folding channels for ribonuclease A; however, additional factors also appear to be involved (Udgaonkar & Baldwin, 1990). These authors suggested that isomerizations at non-proline-containing peptide bonds could be a factor; model studies using *N*-methyl peptides support this hypothesis. Proline isomerization has been ruled out as an explanation for separate folding channels in hen lysozyme (Radford et al., 1992) and DHFR (Jennings et al., 1993).

In the case of DHFR, a potential candidate for a slow isomerization process is the peptide bond between Gly 95 and Gly 96. The X-ray structures of both the MTX binary form (Bolin et al., 1982) and the $NADP^+$/folate ternary form of DHFR (Bystroff et al., 1990) show this peptide bond must be in the *cis* configuration to bind the cofactor. The observed electron density for the apo form of the enzyme, in contrast, is consistent with a mixture of both *cis* and *trans* isomers (Bystroff & Kraut, 1991). Given the location of this peptide bond at the C-terminal end of strand βE and adjacent to Ile 94 (Fig. 1), the different isomeric forms could affect the alignment of this strand within the β-sheet and/or the packing of Ile 94 in the larger hydrophobic cluster. Either perturbation could lead to alternative folding pathways.

Another possible explanation for multiple folding pathways at the stage of the burst phase intermediate of DHFR are the β-bulges (disruptions of the normal hydrogen bonding patterns expected for a β-sheet) at Gly 95, Lys 109, and Phe 137 (Fig. 1). The incorrect formation of any one of these three bulges would lead to alternative, non-native β structures whose amide hydrogens could exchange with solvent as the protein is worked up for NMR analysis. The existence of a β-bulge at Gly 95 could also be related to the isomerization state of the Gly 95–Gly 96 peptide bond.

A third possibility for separate folding channels in DHFR is alternative docking orientations for the adenine binding domain and the larger domain. The two clusters of hydrophobic residues formed in the burst phase intermediate interact with each other through the backbone at strands βB and βE, which define the interface between the two domains (Fig. 5; Bystroff et al., 1990). Mutagenesis studies have already implicated the domain interface as a potential source of the kinetic heterogeneity observed in the later folding reactions (Iwakura et al., 1993). If this hypothesis is correct, the present results suggest that alternative docking arrangements can appear within milliseconds and persist for hundreds of seconds.

General implications for folding

These pulse labeling NMR studies of the folding of DHFR have shown that a network of native hydrogen bonds, which spreads across the β-sheet, appears within 6 ms. The side chains associated with these amide hydrogens form a pair of nonpolar clusters that interact through the backbone in two of the β-strands. When considered with the results of similar studies on the folding of other protein motifs (Udgaonkar & Baldwin, 1988, 1990; Bycroft et al., 1990; Lu & Dahlquist, 1992; Radford et al., 1992; Mullins et al., 1993; Jacobs & Fox, 1994), it is clear that a significant portion of the protein folding problem can be solved within milliseconds for all of the standard motifs. The appearance of both a network of stable hydrogen bonds and hydrophobic clusters in DHFR and other proteins in early folding intermediates suggests that both play important roles in stabilizing these species. It remains to be determined which might dominate even earlier events in folding.

Experimental procedures

Reagents

Ultrapure urea was purchased from ICN and used without further purification; $(^2H)_4$-urea and $K_2{}^2HPO_4$ were prepared by two successive dissolution and lyophilization cycles of the protonated compounds with 99.9% ^2H_2O (Isotech). The MTX affinity reagent was obtained from Sigma and DEAE-Sepharose from Pharmacia. All other chemicals were reagent grade.

Protein purification

Wild-type DHFR (EC 1.5.1.3) was isolated from *E. coli* strain AG-1 (Stratagene) containing the plasmid pWT1-3, as described previously (Jennings et al., 1993). Preparations yielded material that migrated as a single band on both native and SDS-polyacrylamide gels. Protein concentration was determined by using a molar extinction coefficient of $3.11 \times 10^4\ M^{-1}\ cm^{-1}$ (Touchette et al., 1986). Enzymatic activity was monitored by the method of Hillcoat (Hillcoat et al., 1967); the specific activities ranged from 75 to 100 units mg^{-1} in 0.1 M imidazole chloride, pH 7.0, and 30 °C. The reported activity for the wild-type protein is 85 units mg^{-1} under these conditions (Hillcoat et al., 1967).

Hydrogen-deuterium exchange pulse labeling experiments

Pulse labeling experiments were performed at 15 °C in a Bio-Logic QFM-5 rapid-mixing device. DHFR (3 mg mL^{-1}) was denatured and all exchangeable amide hydrogens were deuterated by incubation in 6 M $(^2H)_4$-urea, 50 mM potassium phosphate in 99.9% ^2H_2O (pH* 6.3, uncorrected pH meter reading) at 15 °C for 1 h. Refolding was initiated by rapid sixfold dilution in 50 mM potassium phosphate buffer, pH* 6.3, containing 0.2 mM K_2EDTA and 1 mM β-mercaptoethanol for variable time periods (t_f) prior to the labeling pulse. The labeling pulse was initiated by a twofold dilution into either 200 mM tris-HCl for pulse pH* values below 9.5, or 200 mM glycine for pH* values at and above 9.5; both buffers contained 0.2 mM K_2EDTA and 1 mM β-mercaptoethanol. The final pH values of all steps were checked in independent manual mixing experiments. The labeling was quenched after 20 ms by twofold dilution into 300 mM potassium phosphate, 0.2 mM K_2EDTA and 1 mM β-mercaptoethanol, to a final pH* of 6.3. The deuterium concentrations for the refolding, pulse, and quench steps were 17%, 8%, and 4% respectively. This solution was then injected into a reservoir containing a sufficient amount of folate from a 100 mM stock in 3 mM potassium phosphate (pH 6.8) to provide a 1.5 molar excess to protein and kept on ice. Typically, 25 mg of pulse labeled DHFR was collected by combining the products of ~50 quench flow runs.

An unfolded control ($t_f = 0$) was prepared as above with the exception that both the refolding and pulse buffers contained 6 M urea. A native control ($t_f = \infty$) was prepared by a sixfold dilution of the 6 M $(^2H)_4$-urea/protein solution with 50 mM phosphate buffer in ^2H_2O using manual mixing methods. This mixture was allowed to refold for 1 h at 15 °C, a time sufficient to reach equilibrium in the native conformation. The solution was then placed in the Bio-Logic QFM-5 subjected to a 20-ms pulse at pH* 9.5, quenched, and worked up as described above.

The samples were concentrated and exchanged into degassed 3 mM potassium phosphate, pH 6.8, containing 100 μM folate, by repeated dilution and concentration using an Amicon ultrafiltration cell and a YM-3 membrane. The samples were then concentrated to ~5 mL and a 1.5 molar excess of folate was added from a 100 mM stock. The samples were lyophilized and stored at −70 °C until analysis by NMR. For NMR spectral acquisition, lyophilized samples were dissolved in 450 μL of 99.99% ^2H_2O containing 200 mM KCl.

NMR spectroscopy

Double quantum filtered COSY spectra (Rance et al., 1983) were recorded at 25 °C on a Bruker AM500 NMR spectrometer. The spectral widths were 6,097.1 Hz in both dimensions. A total of 512 t_1 increments, each containing 2K complex points prior to zero-filling in the t_1 dimension and Fourier transformation, were collected. The residual H_2O resonance was suppressed by a 1.2-s low-power presaturation pulse. Data were processed on a Silicon Graphics 240 GTX using the program FTNMR written by Dr. Dennis Hare (Hare Research). Shifted sine-bell windows and gaussian multiplication were used, and the spectra were referenced to H_2O at 4.76 ppm. ^1H NMR assignments were taken from previously published work (Falzone et al., 1990, 1994). Absolute values of the intensities were normalized to three nonexchangeable protons in the aromatic region of the 2QF-COSY spectra. Extent of protonation (proton occupancy) was calculated using the normalized intensities and the values for the unfolded (proton occupancy = 1) and native (proton occupancy = 0) control samples.

Stopped-flow fluorescence experiments

Refolding experiments monitoring tryptophan fluorescence were performed on a Bio-Logic SFM-3 stopped-flow spectrometer (Jennings et al., 1993). The refolding reaction was initiated by a sixfold dilution of DHFR in 6 M urea with buffer (50 mM potassium phosphate, pH 6.3, containing 0.2 mM K_2EDTA and 1 mM β-mercaptoethanol). Tryptophans were excited at 295 nm using a 10-mm slit width and fluorescence emission at wavelengths greater than 325 nm was monitored using a cut-on filter provided by Durrum.

Data analysis

Kinetic data obtained from spectroscopic experiments were fit to a sum of exponentials as previously described (Touchette et al., 1986). Kinetic data obtained from the pulse labeling experiments were fit to a single exponential plus a constant. Data obtained by variation of the pulse pH were fit to an equation expressing the proton occupancy as a function of pH for estimating protection factors (Equation 1, see Results section; Elöve & Roder, 1991). All data fitting was performed using a nonlinear least-squares fitting program, NLIN (SAS Institute Inc., Cary, North Carolina) running on an IBM RS 6000 workstation.

Acknowledgments

We thank Dr. Christopher Falzone for his assistance in acquiring and analyzing the NMR data in the early stages of this work and for providing the assignments prior to publication. We thank Dr. Patricia Jennings for reviewing this manuscript and for many helpful discussions. We also thank Professor George Rose for helpful discussions. This work was supported by a grant from the NSF (MCB 9317273) to C.R.M.

References

Bai Y, Englander SW. 1994. Hydrogen bond strength and β-sheet propensities: The role of a side chain blocking effect. *Proteins Struct Funct Genet 18*:262–266.

Bai Y, Milne JS, Mayne L, Englander SW. 1993. Primary structure effects on peptide group hydrogen exchange. *Proteins Struct Funct Genet 17*: 75–86.

Baldwin RL, Roder H. 1991. Characterizing protein folding intermediates. *Curr Biol 1*:218–220.

Bolin JT, Filman DJ, Matthews DA, Hamlin RC, Kraut J. 1982. Crystal structures of *Escherichia coli* and *Lactobacillus casei* dihydrofolate reductase refined at 1.7 Å resolution. I. General features and binding of methotrexate. *J Biol Chem 257*:13650–13662.

Brandts JF, Halvorson HR, Brennan M. 1975. Consideration of the possibility that the slow step in denaturation reactions is due to *cis–trans* isomerism of proline residues. *Biochemistry 14*:4953–4963.

Briggs MS, Roder H. 1992. Early hydrogen-bonding events in the folding reaction of ubiquitin. *Proc Natl Acad Sci USA 89*:2017–2021.

Bycroft M, Matouschek A, Kellis JT, Serrano L, Fersht AR. 1990. Detection and characterization of a folding intermediate in barnase by NMR. *Nature 346*:488–490.

Bystroff C, Kraut J. 1991. Crystal structure of unliganded *Escherichia coli* dihydrofolate reductase. Ligand-induced conformational changes and cooperativity in binding. *Biochemistry 30*:2227–2239.

Bystroff C, Oatley SJ, Kraut J. 1990. Crystal structures of *Escherichia coli* dihydrofolate reductase: The $NADP^+$ holoenzyme and the folate·$NADP^+$ ternary complex. Substrate binding and a model for the transition state. *Biochemistry 29*:3263–3277.

Cantor CR, Schimmel PR. 1980. *Biophysical chemistry*. New York: W.H. Freeman. pp 145–306.

Creamer TP, Rose GD. 1992. Side-chain entropy opposes α-helix formation but rationalizes experimentally determined helix-forming propensities. *Proc Natl Acad Sci USA 89*:5937–5941.

Creamer TP, Rose GD. 1994. α-Helix-forming propensities in peptides and proteins. *Proteins Struct Funct Genet 19*:85–97.

Elöve GA, Roder H. 1991. Structure and stability of cytochrome *c* folding intermediates. In: Georgiou G, ed. *Protein refolding*. Washington, D.C.: ACS Symposium Series. pp 50–63.

Englander SW, Englander JJ, McKinnie RE, Ackers GK, Turner GJ, Westrick JA, Gill SJ. 1992. Hydrogen exchange measurement of the free energy of structural and allosteric change in hemoglobin. *Science 256*: 1684–1687.

Englander SW, Mayne L. 1992. Protein folding studied using hydrogen exchange labeling and two-dimensional NMR. *Annu Rev Biophys Biomol Struct 21*:243–265.

Falzone CJ, Benkovic SJ, Wright PE. 1990. Partial ^{1}H NMR Assignments of the *Escherichia coli* dihydrofolate reductase complex with folate: Evidence for a unique conformation of bound folate. *Biochemistry 29*: 9667–9677.

Falzone CJ, Cavanagh C, Cowart M, Palmer AG, Matthews CR, Benkovic SJ, Wright PE. 1994. ^{1}H, ^{15}N and ^{13}C resonance assignments, secondary structure, and the conformation of substrate in the binary folate complex of *Escherichia coli* dihydrofolate reductase. *J Biomol NMR 4*: 349–366.

Falzone CJ, Wright PE, Benkovic SJ. 1991. Evidence for two interconverting protein isomers in the methotrexate complex of dihydrofolate reductase from *Escherichia coli*. *Biochemistry 30*:2184–2191.

Hillcoat BL, Nixon PF, Blakley RL. 1967. Effect of substrate decomposition on the spectrophotometric assay of dihydrofolate reductase. *Anal Biochem 21*:178–189.

Itzhaki LS, Evans PA, Dobson CM, Radford SE. 1994. Tertiary interactions in the folding pathway of hen lysozyme: Kinetic studies using fluorescent probes. *Biochemistry 33*:5212–5220.

Iwakura M, Jones BE, Falzone CJ, Matthews CR. 1993. Collapse of parallel folding channels in dihydrofolate reductase from *Escherichia coli* by site-directed mutagenesis. *Biochemistry 32*:13566–13574.

Jacobs MD, Fox RO. 1994. Staphylococcal nuclease folding intermediate characterized by hydrogen exchange and NMR spectroscopy. *Proc Natl Acad Sci USA 91*:449–453.

Jennings PA, Finn BE, Jones BE, Matthews CR. 1993. Reexamination of the folding mechanism of dihydrofolate reductase from *Escherichia coli*: Verification and refinement of a four channel model. *Biochemistry 32*: 3783–3789.

Jennings PA, Wright PE. 1993. Formation of a molten globule intermediate early in the kinetic folding pathway of apomyoglobin. *Science 262*: 892–896.

Jones BE, Beechem JM, Matthews CR. 1995. Local and global dynamics during the folding of *Escherichia coli* dihydrofolate reductase by time-resolved fluorescence spectroscopy. *Biochemistry 34*:1867–1877.

Jones BE, Jennings PA, Pierre RA, Matthews CR. 1994. The development of nonpolar surfaces in the folding of dihydrofolate reductase from *Escherichia coli*. *Biochemistry 33*:15250–15258.

Jones CM, Henry ER, Hu Y, Chan C, Luck SD, Bhuyan A, Roder H, Hofrichter J, Eaton WA. 1993. Fast events in protein folding initiated nanosecond laser photolysis. *Proc Natl Acad Sci USA 90*:11860–11864.

Khorasanizadeh S, Peters ID, Butt TR, Roder H. 1993. Folding and stability of a tryptophan-containing mutant of ubiquitin. *Biochemistry 32*: 7054–7063.

Kim CA, Berg JM. 1993. Thermodynamic β-sheet propensities measured using a zinc-finger host peptide. *Nature 362*:267–270.

Kuwajima K. 1989. The molten globule state as a clue for understanding the folding and cooperativity of globular protein structure. *Proteins Struct Funct Genet 6*:87–103.

Kuwajima K, Garvey EP, Finn BE, Matthews CR, Sugai S. 1991. Transient intermediates in the folding of dihydrofolate reductase as detected by far-ultraviolet circular dichroism spectroscopy. *Biochemistry 30*:7693–7703.

Lu J, Dahlquist FW. 1992. Detection and characterization of an early folding intermediate of T4 lysozyme using pulsed hydrogen exchange and two-dimensional NMR. *Biochemistry 31*:4749–4756.

Lumb KJ, Carr CM, Kim PS. 1994. Subdomain folding of the coiled coil leucine zipper from the bZIP transcriptional activator GCN4. *Biochemistry 33*:7361–7367.

Mann CJ, Matthews CR. 1993. Structure and stability of an early folding intermediate of *Escherichia coli trp* aporepressor measured by far-UV stopped-flow circular dichroism and 8-anilino-1-naphthalene sulfonate binding. *Biochemistry 32*:5282–5290.

Minor DL, Kim PS. 1994. Measurement of the β-sheet-forming propensities of amino acids. *Nature 367*:660–663.

Mullins SL, Pace CN, Raushel FM. 1993. Investigation of ribonuclease T_1 folding intermediates by hydrogen-deuterium amide exchange—Two-dimensional NMR spectroscopy. *Biochemistry 32*:6152–6156.

Radford SE, Dobson CM, Evans PA. 1992. The folding of hen lysozyme involves partially structured intermediates and multiple pathways. *Nature 358*:302–307.

Rance M, Sørenson OW, Bodenhausen G, Wagner G, Ernst RR, Wüthrich K. 1983. Improved spectral resolution in COSY-^{1}H NMR spectra of proteins via double quantum filtering. *Biochem Biophys Res Commun 117*: 479–485.

Roder H, Elöve GA, Englander SW. 1988. Structural characterization of folding intermediates in cytochrome *c* by H-exchange labeling and proton NMR. *Nature 335*:700–704.

Semisotnov GV, Rodionova NA, Razgulyaev OI, Uversky VN, Gripas AF, Gilmanshin RI. 1991. Study of the "molten globule" intermediate in protein folding by a hydrophobic fluorescent probe. *Biopolymers 31*:119–128.

Shin HC, Merutka G, Waltho JP, Tennant LL, Dyson HJ, Wright PE. 1993. Peptide models of protein folding initiation sites. 3. The G-H helical hairpin of myoglobin. *Biochemistry 32*:6356–6364.

Smith CK, Withka JM, Regan L. 1994. A thermodynamic scale for the β-sheet forming tendencies of the amino acids. *Biochemistry 33*:5510–5517.

Sugawara T, Kuwajima K, Sugai S. 1991. Folding of staphylococcal nuclease A studied by equilibrium and kinetic circular dichroism spectra. *Biochemistry 30*:2698–2706.

Touchette NA, Perry KM, Matthews CR. 1986. Folding of dihydrofolate reductase from *Escherichia coli*. *Biochemistry 25*:5445–5452.

Udgaonkar JB, Baldwin RL. 1988. NMR evidence for an early framework intermediate on the folding pathway of ribonuclease A. *Nature 335*: 694–699.

Udgaonkar JB, Baldwin RL. 1990. Early folding intermediate of ribonuclease A. *Proc Natl Acad Sci USA 87*:8197–8201.

Varley P, Gronenborn A, Christensen H, Wingfield PT, Pain RH, Clore GM. 1992. Kinetics of folding of the all-β sheet protein interleukin-1β. *Science 260*:1110–1113.